Molecular dynamics simulations of temperature-induced structural transitions at twist boundaries in silicon

S. von Alfthan,[1,2] K. Kaski,[1] and A. P. Sutton[3]
[1]*Helsinki University of Technology, Laboratory of Computational Engineering, P.O. Box 9203, FIN 02015 HUT, Finland*
[2]*CSC—Scientific Computing, Ltd., P.O. Box 405, FIN 02101 Espoo, Finland*
[3]*Imperial College London, Department of Physics, Exhibition Road, London SW7 2AZ, United Kingdom*
(Received 24 August 2007; published 18 December 2007)

The annealing of three (001) twist grain boundaries in silicon, $\Sigma 25$, $\Sigma 5$, and $\Sigma 29$ has been simulated over a range of temperatures up to the melting point. In contrast to earlier work the ground-state structures of all our boundaries at absolute zero are ordered and comprise well-defined structural units. We found that the boundaries display some degree of structural order at all temperatures up to the melting point. The state of structural order is time-dependent involving fluctuations between different local states of order. In the large angle boundaries ($\Sigma 5$ and $\Sigma 29$) we found a continuous disordering transition resulting in complete disorder, and a possibly unbounded interfacial width, only at the bulk melting point. For the small angle $\Sigma 25$ boundary the width remained finite at all temperatures up to the bulk melting point, and the degree of order was greater than for the large angle boundaries. The quantification of these results has been made possible by the use of an existing bond orientational order parameter, and new techniques introduced here to identify structural units in dynamic boundary structures.

DOI: 10.1103/PhysRevB.76.245317 PACS number(s): 61.72.Mm, 82.20.Wt, 68.35.Ct

I. INTRODUCTION

The structures of grain boundaries (GBs) influence and may even dominate the mechanical and electronic properties of polycrystalline materials.[1] There has been a long-standing interest in the thermal stability of GB structures, notably in the possibility of transitions as the temperature is raised accompanied by disordering and widening of the interface. For a recent review of experiments and simulations in this area, see Tang *et al.*[2]

Recently we revisited the question of the ground-state structures of (001) twist GBs in silicon.[3,4] In these studies, as compared with earlier work, we enlarged the sampling of the configuration space of the boundaries, both by removing atoms from the boundary plane and by carrying out simulated anneals that were longer by up to two orders of magnitude. We found new configurations for these boundaries as being characterized by significantly more structural order and smaller energy than those found earlier. Our results were obtained with an empirical potential for silicon constructed by Tersoff,[5] and those for the smallest period twist boundary were confirmed by first principles electronic density functional calculations. In this paper we study three of these boundary structures by annealing them up to the melting point and examine the changes in their structural order. We find similarities but also significant differences compared with earlier work[6] on annealing these boundaries in silicon. These differences arise primarily because our initial, low temperature configurations are more ordered than those obtained before.

A thermodynamic analysis has been presented recently by Tang *et al.*[2] for the variation of the degree of structural order in a GB in a single component system, as a function of temperature and misorientation about a fixed axis. This theory is based on a phase-field representation of the free energy of a GB involving a functional of the "degree of crystallinity" as a gradient expansion.

The theory predicts three types of behavior. In a range of intermediate misorientations, and a range of temperatures below the bulk melting point T_M, a first order phase transition may occur. We call this type 1 behavior. At such a transition the degree of structural order changes discontinuously from a more ordered state below the transition temperature to a more disordered state above it. At the same time the structural width of the boundary changes discontinuously. On heating further the boundary disorders more and its width increases until the boundary is replaced by a perfectly wetting liquid at T_M.

Type 2 behavior may arise on heating relatively large energy (often large angle) boundaries: the disorder and width of the boundary increase continuously without passing through a first order phase transition. As the temperature approaches T_M the structural order again decreases continuously to that of a bulk liquid, and the boundary width diverges.

Type 3 behavior may arise on heating relatively small energy (often small angle) boundaries: the disorder increases without passing through a first order phase transition, but as the temperature approaches T_M the degree of structural order remains greater than that of the bulk liquid. The boundary width also remains finite as the temperature approaches T_M.

A tenet of this thermodynamic analysis[2] is that boundaries may display partial order, i.e., they have structures intermediate between those of bulk liquids and single crystals. However, no attempt was made to define what that means in terms of the atomic structure of the boundary. The lack of such a satisfactory definition was identified[2] as "a challenge for materials simulators, theorists and experimentalists." In this work we make extensive use of two characterizations of structural order at a boundary. One of them is an order parameter which we used[3,4] to distinguish between atoms in the boundary and the perfect crystal to determine the widths of boundaries. Secondly, we define a new order parameter as the fraction of atoms in the boundary associated with

predefined structural units. This order parameter enables us to quantify the change in the structural order of the boundary due to heating, but also to examine quantitatively fluctuations in this ordered state. With this order parameter we find that our simulations display both types 2 and 3 behavior, but we find no evidence of type 1 behavior.

We simulate the heating to the melting point of three (001) twist boundaries Σ25, Σ5, and Σ29, with misorientations of ≈16°, 37°, and 44°, respectively. The initial configurations are minimum energy structures at 0 K obtained in Refs. 3 and 4. The large-angle Σ5 boundary structure comprises two structural units *A* and *B* (Fig. 1). The small-angle Σ25 boundary has the same two structural units *A* and *B* located at the intersections of a square grid of $\frac{1}{2}\langle 110\rangle$ screw dislocations, which lie along the diagonals of the dashed box in Fig. 1. In between the screw dislocation cores there are patches of elastically strained crystal. The large-angle Σ29 boundary structure comprises several structural units (Fig. 1). In addition to the *B* unit we have identified several new structural units (see the caption to Fig. 1): the *T* and *X* units comprise three and four five-membered rings, respectively. In each primitive cell there are two *T* and two *X* units. In addition, there are two *M* units per primitive cell. The identification of these structural units is based on the observation that although they undergo structural fluctuations at elevated temperatures they are nevertheless reformed, at least until the boundary disorders completely. We view their repeated disappearance and reappearance until the boundary completely disorders as evidence of their structural significance.

II. COMPUTATIONAL METHODS

We have carried out molecular dynamics (MD) simulations using the Tersoff III (TS) potential[5] at constant total volume and temperature. The temperature was controlled by a Nose-Hoover thermostat[7] and the duration of the simulations was between 30 and 50 ns with a time-step of 1 fs. These long simulation times were necessary to get adequate statistics. At each temperature we set the crystal lattice parameter to be that which gave zero net pressure for bulk crystalline Si, as obtained with the Tersoff potential. To reduce thermal noise the atomic positions were averaged over 300 fs time intervals and the atomic configurations were stored every 10 ps for statistical analysis.

The computational supercells comprised 2×2 primitive repeat cells in the GB plane for Σ25 and Σ29 boundaries, and 4×4 primitive cells for the Σ5 boundary. There were 50 Å thick slabs of crystalline Si on either side of the GB with free surfaces parallel to the GB plane. In the simulations performed at temperatures close to the melting point the thickness of the slabs was 200 Å. The free surfaces allowed the GB to adjust its density freely, and to adopt any relative rigid-body translation parallel to the boundary plane. Periodic boundary conditions were applied in all the three directions with no further changes in the dimensions of the computational supercell after the initial adjustment for the crystal lattice parameter at each temperature. In the direction normal to the boundary plane there was sufficient vacuum between the slabs such that the free surfaces were not interacting. In

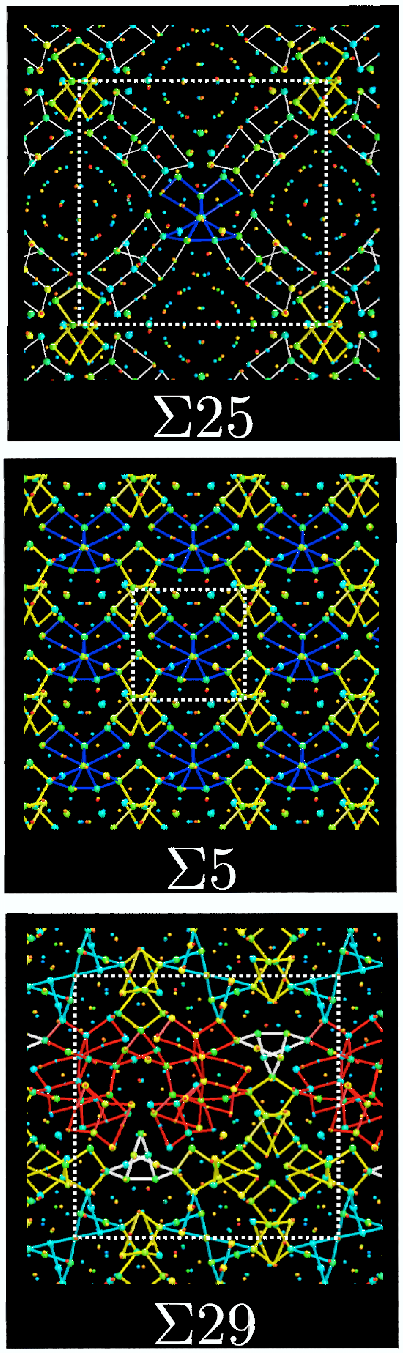

FIG. 1. (Color online) Minimum energy structures of Σ25, Σ5, and Σ29 (001) twist boundaries at 0 K (Refs. 3 and 4). The boundaries are shown in plan view. The white dashed boxes outline one primitive repeat cell. Bonds in only five-membered rings are drawn and their coloring identifies the structural unit to which they belong. Blue bonds belong to *A* units, yellow to *B* units, and in the Σ25 boundary white thin bonds outline the $\frac{1}{2}\langle 110\rangle$ screw dislocation cores. In the Σ29 boundary white thick bonds belong to *T* units, light blue to *X* units and red bonds to *M* units. The two *M* units in each primitive cell are adjacent and share three atoms. The coloring indicates position along the boundary normal, blue atoms or bonds are further from the viewer while red atoms or bonds are closer. The larger atoms are within the GB core region, whereas the smaller atoms are in the adjacent crystals.

the simulations of the two large angle boundaries, performed at temperatures close to the melting point, the GB became wide and highly mobile, and there was a risk that it would collide with one of the free surfaces. To ensure that our results were not influenced by the surfaces we terminated simulations once the GB had moved more than halfway through one of the crystalline slabs on either side of the boundary. In practice this set an upper limit on the temperature we were able to simulate for these boundaries.

In order to identify atoms in the GB we used a bond orientational order parameter.[3,8] This parameter is a measure of the correlation between the angular distribution of the bonds to an atom and the angular distribution of the bonds to its neighbors. At all temperatures, two atoms are considered bonded if they are within 2.85 Å of each other. This corresponds to the approximate position of the first minimum in the radial distribution function. The order parameter is unity in a perfect crystal and tends to zero in a completely disordered solid. We define atoms in the GB to be those which have an order parameter less than 0.7, or those which are bonded exclusively to such atoms. We have found that this choice conveniently identifies atoms forming the GB core. A consequence of this definition is that for the Σ25 boundary atoms in the elastically strained crystal patches between the screw dislocations are not designated as being part of the GB because the local order parameter is above 0.7.

The existence of structural units is an indication of structural order at a GB because it implies certain preferred atomic configurations are adopted. The reappearance of structural units after they have disappeared through a thermal fluctuation is evidence that they are energetically favorable configurations in the GB. If that were untrue then the probability of them reappearing would be negligible on the time scale of a molecular dynamics simulation. Secondly, the existence of the same structural unit, albeit in a slightly distorted form, in boundaries nearby in the misorientation range is further evidence that it is a favorable configuration.[9]

We have developed an algorithm to identify structural units in the GB through comparisons with ideal units at 0 K. To do this at elevated temperatures we use several criteria which permit modest deviations from the atomic configurations of the ideal units at 0 K. The criteria are applied to five-membered rings comprising a candidate atomic configuration and those comprising an ideal unit. For a five-membered ring in the candidate structure to be identified with a particular ring in the ideal unit the root mean square difference of the order parameters of the atoms in the two rings has to be less than 0.22. In addition, the angle between the normals to the rings has to be smaller than 15°. As five-membered rings are not quite planar the plane of the ring is found by minimization of the mean square deviation of the plane from the positions of the five atoms comprising the ring. Some rings in the ideal structural unit are connected to each other through shared atoms. The number and relative locations of the connecting atoms have to match in the ideal unit and the candidate structure. We also require that the distance between the centers of mass of two rings in the candidate structure is within 10% of the corresponding value in the ideal unit. Finally, the angles between normals to rings in the candidate structure have to be within 15° of the corresponding values in the ideal unit. The values of all these tolerances have been found by trial and error to yield meaningful results.

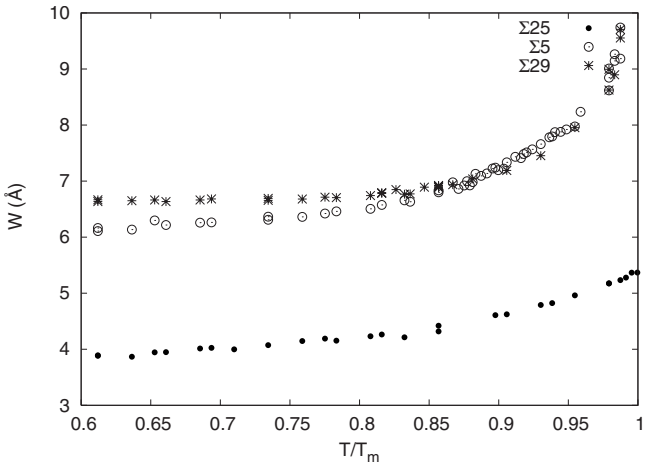

FIG. 2. The average width of the GB as a function of the homologous temperature.

In addition to classifying atoms as being in the GB or in the adjacent crystals, we associate atoms in the GB with either ordered or disordered regions. Ordered regions in our boundaries are defined by structural units present in the ground-state boundary structures at 0 K and a small number of metastable structural units that appear in higher energy boundary configurations. These structural units are all characterized by five-membered rings. Any atom in a five-membered ring that is part of such a structural unit is classified as "ordered," by which we mean it is associated with an ordered region. We classify any atom bonded directly to these atoms also as ordered because the locations of nearest neighbors of atoms comprising structural units are also well defined. All other atoms in the GB are classified as "disordered." The result of this classification scheme is that at 0 K all atoms in the GB are designated as "ordered."

The planar diffusivity of atoms in each region is calculated using the mean-square distance over which atoms move during a time interval t:

$$D = \frac{1}{4}\frac{\partial\langle r^2(t)\rangle}{\partial t}, \tag{1}$$

where D is the diffusion constant and $r(t)$ is the distance that an atom moves parallel to the GB in a time t. We calculate D for time intervals up to 300 ps. During this interval the designated state of order for the atom must not change in order to contribute to $\langle r^2(t)\rangle$. As the temperature rises the lifetime of ordered states decreases, and it is then no longer possible to calculate the diffusivity for ordered states. Subject to the same limitation we have also calculated the bond angle distributions in both ordered and disordered regions.

To characterize the profile of a GB we calculate the surfaces separating atoms defined to be in the GB and those in the adjacent crystals using the Voronoi construction. These surfaces enable us to calculate the mean width W of the boundary (Fig. 2). Since the adjacent crystals penetrate

through patches of the Σ25 boundary these regions have zero boundary width.

The melting point of crystalline Si differs in our model from that of real Si partly because we are using a thin slab geometry and partly because we are using an empirical potential for Si. We have computed the melting point T_M with the Tersoff potential for a single crystal slab of the same dimensions as our bicrystals as follows. We annealed the slab at 2800 K, which is far above T_M, for a short period until approximately half the slab had melted from the free surfaces. We then annealed the slab at a number of temperatures below 2800 K and calculated the rate at which the order parameter, summed over all atoms, changed with time. An increase of the order parameter indicated the annealing temperature was below T_M, a decrease indicated it was above T_M. By linear interpolation the melting temperature was found to be $T_M=2451\pm1$ K. The melting point of a real slab of crystalline Si of these dimensions would be less than the true melting point of bulk Si, i.e., 1670 K. The value we obtained is significantly higher because of limitations of the Tersoff potential model. In the following we normalize all our temperatures to $T_M=2451$ K to make comparisons with other simulations and experiments.

We have calculated structural and physical properties of amorphous Si at crystalline densities to compare with those of the GB core regions. A supercell containing 512 atoms of crystalline Si at the 0 K lattice parameter was annealed at 3500 K for 100 ps at constant volume, with periodic boundary conditions in all three directions. This temperature lies well above the melting point and the crystal melted. The sample was cooled to 0 K at 0.23 K/ps at constant volume which resulted in a well-equilibrated supercell of low density amorphous silicon. Structural and physical properties of low density amorphous silicon were calculated at selected temperatures by carrying out further anneals each of 10 ns duration. The density of the supercell was set to the crystalline density at each of these temperatures.

III. RESULTS

In Fig. 2 we plot the boundary widths, as determined by the procedure involving the order parameter to identify atoms of the GB core and the Voronoi construction for the surfaces separating the GB core from the perfect crystal. The width (Fig. 2) of the Σ25 boundary increases by ≈0.1 nm but remains finite up to the melting point. For both Σ5 and Σ29 boundaries the width increases sharply as the temperature approaches the melting point and may become unbounded at the melting point. At temperatures above $T=0.85T_M$ the widths of the Σ5 and Σ29 boundaries coincide which suggests that the structures of the two large angle boundaries becomes similar.

The atomic density of the boundary is one method that has been used[6] for detecting GB structural transitions on heating. Normal liquid silicon is sixfold coordinated and is significantly denser than either crystalline or amorphous silicon. Therefore, we should be able to detect a significant change of density if the boundary transforms to a high density liquid. The density of the boundary has been studied[6]

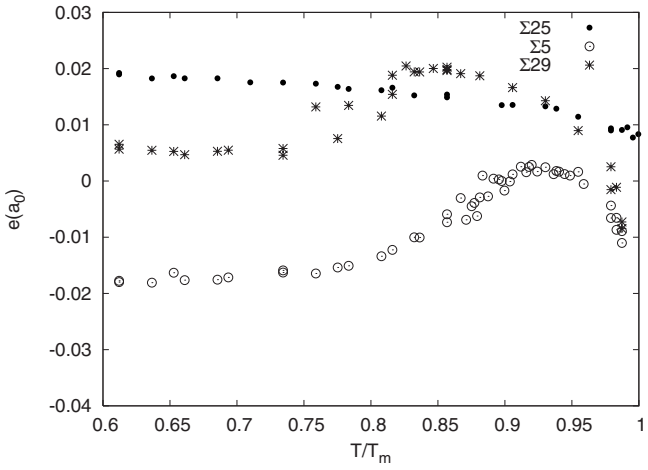

FIG. 3. Expansions in units of the lattice constant at temperature T of the three (001) twist GBs as a function of the homologous temperature.

through the expansion e of the GB which is defined as the excess volume of the GB per unit area:

$$e = \frac{V_{\mathrm{GB}r} - V_{\mathrm{cr}}}{A}, \tag{2}$$

where $V_{\mathrm{GB}r}$ is the volume of a region containing all atoms within the boundary, as defined by the order parameter, and four atomic layers of crystal either side of the GB, and V_{cr} is the volume of a region of perfect crystal containing the same number of atoms at the same temperature. As with all excess quantities the boundary expansion is independent of the volume sampled provided it includes all the material that is affected by the presence of the GB. In Fig. 3 we have plotted e for each GB as a function of temperature. The expansion of the Σ25 boundary decreases slightly and monotonically with temperature, reaching a value of almost zero at the melting point. The expansions of the Σ5 and Σ29 boundaries are more interesting showing the onset of a rise in the expansion at about $0.8T_M$ which peaks before falling rapidly as T approaches T_M.

The atomic density of the boundary may be defined as $n_{\mathrm{GB}}/V_{\mathrm{GB}}$, where n_{GB} is the number of atoms in the volume V_{GB} of the boundary. Using the boundary widths we have calculated V_{GB} and hence the densities of the boundaries as shown in Fig. 4. For the Σ25 boundary the density remains essentially constant at about 7% less than that of the perfect crystal. For the Σ5 boundary the density is slightly greater than that of the perfect crystal at low temperatures, decreasing slowly with temperature until $T\approx0.8T_M$. The density then starts to decrease more rapidly, reaching a minimum at $T\approx0.95T_M$ above which it increases rapidly but remains less than that of crystalline Si. The variation of the density of the Σ5 boundary with temperature reflects the variation of the expansion of this boundary. In the case of the Σ29 boundary the density slowly increases up to about $T=0.95T_M$, above which it increases more rapidly but remains less than that of the perfect crystal. This behavior is quite different from that reported in Ref. 10 for the Σ29 (001) twist GB in Si. As we

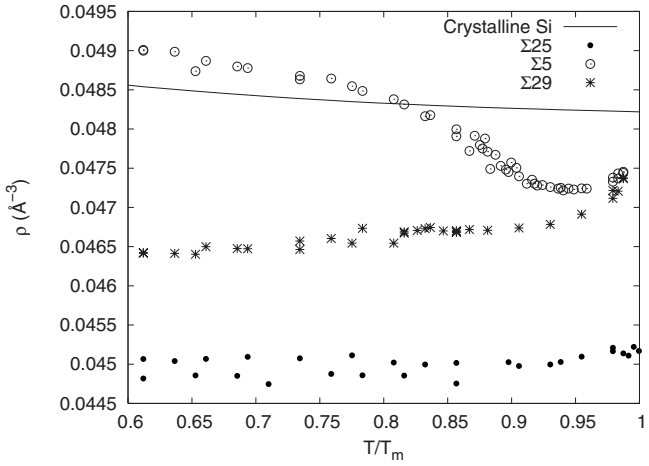

FIG. 4. The atomic density of the three (001) twist GBs as a function of the homologous temperature.

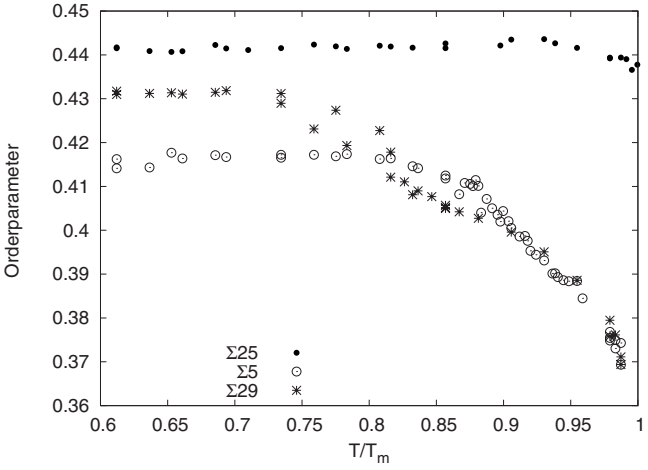

FIG. 6. The average order parameter of atoms in the GBs as a function of the homologous temperature.

note below, the reason for this difference is that our 0 K GB has a significantly lower energy and greater structural order than that obtained in Ref. 10.

The time-averaged fractions of atoms in the GBs designated as being ordered are plotted in Fig. 5. They show that the onset of the rises in the corresponding boundary expansions seen in Fig. 3 correlate with the temperatures at which the fractions of ordered atoms start to decrease. In the cases of the $\Sigma 5$ and $\Sigma 29$ boundaries it is only at the melting point that structural units have permanently disappeared. The average order parameter of atoms designated as being in the boundary core is shown in Fig. 6 as a function of temperature. This will always be finite at temperatures below T_M because atoms are defined to be in the GB if their order parameter is less than 0.7 or if they are bonded exclusively to such atoms. Nevertheless, we see in Fig. 6 a reduction in the time-average order parameter for the $\Sigma 5$ and $\Sigma 29$ boundaries which begins at temperatures comparable to the onset of the reduction of order seen in Fig. 5 for these boundaries. These trends are consistent with the variation in the potential energy of the boundaries with increasing temperature shown in Fig. 7.

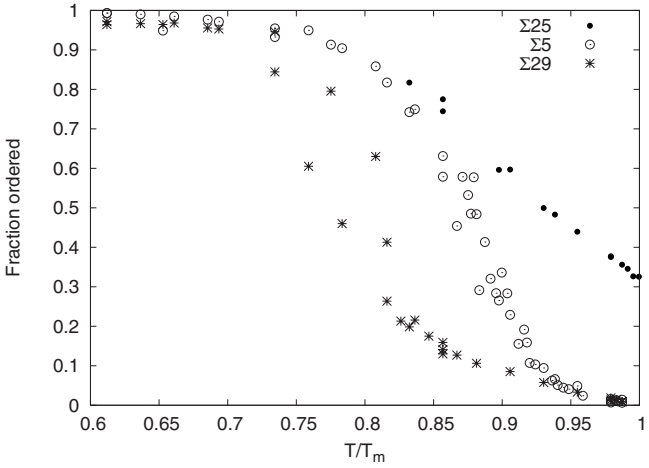

FIG. 5. The fraction of the GBs that is ordered as a function of the homologous temperature.

The time averaging required to generate Figs. 5–7 hides an interesting aspect of the disordering process. Animations of the dynamical simulations of the $\Sigma 5$ boundary show that *A* units may transform into *B* units and vice versa. This happens because *A* and *B* units are remarkably close to each other structurally: just two atoms have to move by approximately 1.2 Å to change one unit into the other. In addition, *A* and *B* units may disorder temporarily before subsequently reordering as either *A* or *B* units. Thus the ground-state structure of the $\Sigma 5$ boundary fluctuates into other ordered states with higher potential energies. Some of the new ordered states are closely related to the metastable higher energy states we found at 0 K for $\Sigma 5$ boundaries comprising 2×2 primitive cells in Ref. 4. The temperature-induced disordering process is dynamical: a given patch of the boundary fluctuates between ordered and disordered states, with the frequency of the fluctuations increasing approximately exponentially, as will be shown below. This is quite different from a picture of the disordering process involving the nucleation of a permanently disordered (amorphous or liquid) region that grows with increasing temperature, eventually con-

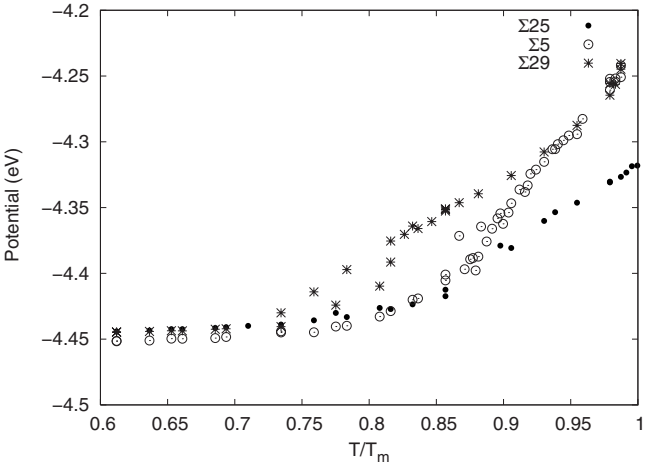

FIG. 7. The average potential energy of atoms in the GBs as determined by the Tersoff III (Ref. 5) potential as a function of the homologous temperature.

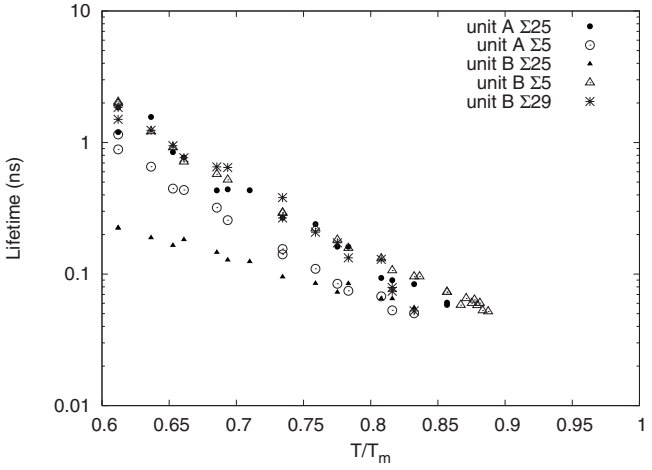

FIG. 8. The lifetimes of A and B units in GBs as a function of the homologous temperature. The boundary structure is sampled every 10 ps. This may lead to an overestimate of the lifetime if a unit disappears and reappears between successive frames. For this reason only lifetimes calculated to be at least five times the sample period, i.e., 50 ps, are shown.

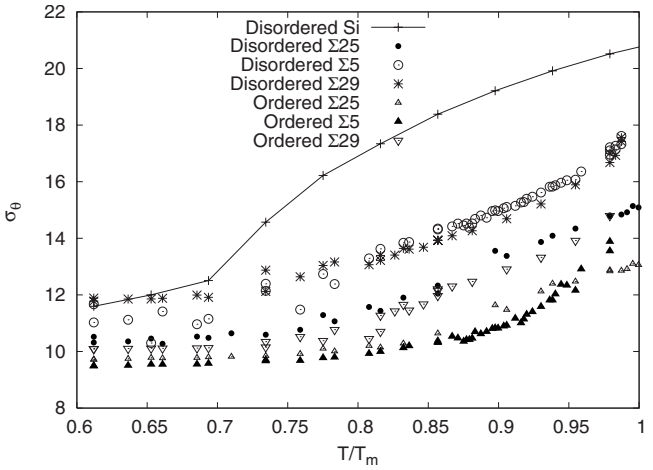

FIG. 9. The time average widths σ_θ of the distributions of bond angles in degrees for the ordered and disordered regions of the three GBs as a function of the homologous temperature. Also shown is the variation of σ_θ for low density amorphous and supercooled liquid silicon.

suming the entire boundary. The dynamical disordering process in the $\Sigma 29$ boundary is similar to that in the $\Sigma 5$ boundary, although the tendency for structural units to transform into each other is more limited, and A units are virtually absent at all temperatures in the $\Sigma 29$ boundary. For the $\Sigma 25$ boundary A and B units undergo similar transformations as in the $\Sigma 5$ boundary. The crystalline patches between the screw dislocation cores remain stable to the melting point, which explains the behavior of this boundary seen in the figures.

To characterize further the dynamical nature of the disordering process we have determined average lifetimes of structural units as a function of temperature, see Fig. 8. We see that the lifetimes decrease rapidly with increasing temperature, and tend towards 10 ps at the melting point. This confirms that structural units are present at all temperatures up to the melting point. Even though structural units have increasingly transitory existences with increasing temperature, the boundary returns to them at all temperatures up to the melting point. It is as if the boundary retains a memory of its ordered configurations throughout the disordering process up to the melting point.

Having distinguished between ordered and disordered regions of a GB, and noted their transitory existences, we seek to characterize them further. Disordered regions and ordered regions coexist in the boundary and one may wonder how much these "disordered" regions resemble amorphous or supercooled liquid silicon. We address this question in two ways, one structural the other physical.

In Fig. 9 the time-averaged widths σ_θ of the distributions of bond angles to atoms in the disordered and ordered regions have been plotted. σ_θ is larger for the disordered than the ordered regions, which is consistent with disordered regions corresponding to larger deviations from the crystalline state. The disordered regions in the $\Sigma 29$ and $\Sigma 5$ boundaries have similar values of σ_θ suggesting these regions are structurally similar. The disordered regions in the $\Sigma 25$ boundary have a smaller σ_θ than those in the $\Sigma 5$ and $\Sigma 29$ boundaries at all temperatures, as expected for screw dislocations confined by regions of elastically strained crystal. The ordered regions of the $\Sigma 25$ and $\Sigma 5$ boundaries have very similar spreads of bond angles, which is consistent with them both being formed from A and B units (it will be recalled that the elastically strained perfect crystal regions in the $\Sigma 25$ boundary are excluded from the boundary because the order parameter is greater than 0.7). The ordered regions in the $\Sigma 29$ boundary have higher values of σ_θ than ordered regions in the other two boundaries, consistent with the higher energy of the former boundary.

The curve of σ_θ for low density amorphous silicon shows a marked kink at $T/T_M \approx 0.7$ which we interpret as the onset of a continuous glass transition in low density amorphous silicon to low density supercooled liquid silicon. Evidence for such a transition has been found experimentally.[11] At temperatures above $T/T_M \approx 0.7$ the value of σ_θ for low density supercooled liquid silicon is significantly greater than that for any boundary disordered regions. It follows that the disordered boundary regions at temperatures above $T/T_M \approx 0.7$ are not structurally similar to low density supercooled liquid silicon.

The structural distinctions between disordered and ordered boundary regions, and between disordered boundary regions and low density supercooled liquid silicon, are supported by the physical characterization of these regions based on the atomic diffusivities. In Fig. 10 we have plotted the log of the in-plane self-diffusivities of ordered and disordered regions of the three boundaries against the inverse temperature. The diffusivities in bulk low density supercooled liquid (high T) and in amorphous Si (low T) have also been plotted for comparison. We see that the diffusivities of all boundary regions are significantly less than that of low density amorphous silicon at low temperatures and supercooled liquid silicon at high temperatures. This indicates that the atomic mobilities in the disordered boundary regions are never as high as those in bulk amorphous and supercooled liquid silicon.

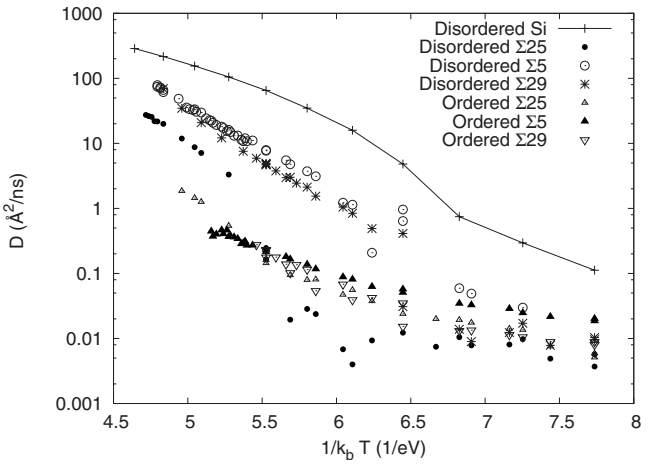

FIG. 10. The diffusivities of ordered and disordered regions of the Σ25, Σ5, and Σ29 boundaries. The diffusivity of bulk low density amorphous and supercooled liquid Si is also shown.

There is a marked difference between the diffusivities of the ordered and disordered regions especially at high temperatures. The disordered regions of the Σ29 and Σ5 boundaries have similar diffusivities, and they become indistinguishable as the temperature approaches T_M. The activation energies and the preexponential factors of the diffusivities are given in Tables I and II.

IV. DISCUSSION

We have sought to define the degree of order in a GB in two ways. First, the bond orientational order parameter[3,8] provides a quantitative and continuous measure of the degree of order of the environment of an atom. It does so by calculating the correlation between the orientations of the bonds to the nearest neighbors of the atom and the orientations of bonds to the next nearest neighbors. It has been used here to distinguish between environments of atoms in the GB core and in the perfect crystal, and thus to distinguish between "GB atoms" and "crystal atoms." Second, we have identified structural units which make up the three boundaries at 0 K. These structural units enabled us to identify GB atoms as being either "ordered" or "disordered," as described in Sec. II. The fraction of GB atoms that are ordered is a measure of the partial order of the boundary and it has been plotted in Fig. 5 as a function of temperature.

We have presented properties of Σ25, Σ5, and Σ29 (001) twist boundaries in Si at temperatures ranging from $0.6T_M$ up to T_M. The expansion (Fig. 3), the width (Fig. 2), the fraction ordered (Fig. 5), the order parameter (Fig. 6), and the average potential energy (Fig. 7) all indicate that the large angle GBs (Σ5 and Σ29) undergo continuous transitions that start at around $0.7-0.8T_M$. Since the widths of these boundaries appear to diverge at T_M the transition is of type 2. However, both the widths of the bond angle distributions (Fig. 9) and the diffusivity (Fig. 10) indicate that the structures of these boundaries transform into something that may *not* be described as low density supercooled liquid silicon. In Fig. 4 we see that at temperatures between $0.6T_M$ and T_M the densities of the boundary cores are *less* than, or only slightly greater than, that of crystalline silicon. These results are in marked conflict with those obtained by Keblinski *et al.*[6] for the Σ29 (001) twist boundary in Si. The principal reason for this difference is that at 0 K our Σ29 boundary structure is more ordered and it has a smaller energy[4] than the 0 K configurations obtained by Keblinski *et al.*[6] The difference in the degree of order in the boundary structures at 0 K is so large that it leads to qualitatively different mechanisms in introducing disorder into the boundaries when heated.

When the Σ25 boundary is heated to the melting point the ordered fraction remains finite (Fig. 5), the boundary expansion decreases gradually (Fig. 3), the average bond orientational order parameter (Fig. 6), and the density of the GB core (Fig. 4) change very little. The boundary width increases gradually on heating without diverging close to T_M. When melting occurs at $T=T_M$ it is initiated at the free surfaces. One might wonder whether there is any transition at all at this boundary on heating, but there is a marked change in the diffusivity parameters at high temperatures, as seen in Fig. 10, and the average potential energy begins to increase more rapidly at about $0.8T_M$ (Fig. 7). We believe, therefore, that this is an example of a type 3 transition.

On heating these boundary structures we find that structural disorder is introduced through fluctuations between different locally ordered states and between locally ordered and disordered states. These transitions between different local atomic configurations are the source of the increase in the configurational entropy of the boundary. We emphasize that the disordering mechanism is quintessentially time dependent.

The diffusivities (Fig. 10) of atoms in disordered environments of the Σ5 and Σ29 boundaries are significantly smaller than that of bulk low density liquid or amorphous Si, and these diffusivities appear to converge only at the melting point. Together with the data on the widths of the bond angle distributions in Fig. 9 this provides evidence that the boundary structure does not transform into a low density supercooled liquid when it disorders at any temperature below T_M.

TABLE I. Activation energy E_a and prefactor $\ln(D_0)$ for the diffusivity of disordered atoms.

	T/T_M	E_a (eV)	$\ln(D_0)[\ln(\text{Å}^2/\text{ns})]$
Σ25	0.90–1.0	3.8±0.09	21.2±0.4
Σ5	0.75–1.0	3.1±0.04	19.1±0.2
Σ29	0.75–1.0	3.4±0.08	20.1±0.5
Σ25	0.60–0.80	0.2±0.2	−3.6±1.3

TABLE II. Activation energy E_a and $\ln(D_0)$ for the diffusion constant of ordered atoms, where D_0 is the preexponential factor.

	T/T_m	E_a (eV)	$\ln(D_0)[\ln(\text{Å}^2/\text{ns})]$
Σ25	0.75–1.0	3.2±0.2	16.1±1.3
Σ5	0.75–1.0	1.9±0.05	8.8±0.3
Σ29	0.75–1.0	2.5±0.3	12.2±1.5

There is an increase in both the activation energy and activation entropy, which is contained in the preexponential factor, for diffusion in the disordered regions of $\Sigma 5$ and $\Sigma 29$ boundaries at $T=0.7T_M-0.8T_M$. This implies a change of mechanism of diffusion to one involving coordinated movements of groups of atoms at higher temperatures. For example, it is possible that it coincides with a transition from atomic transport in disconnected disordered islands to transport in a percolating network of disordered regions that allows atoms to move greater distances. For the $\Sigma 25$ boundary there is a similar increase of activation energy and activation entropy for diffusion at higher temperatures.

The roughening transition at free surfaces and grain boundaries is also characterized by thermal fluctuations of an underlying ordered structure that result in an increase in the boundary width. It is also not a premelting transition,[1] and is primarily characterized by the disappearance of facets on heating. It is only by investigating nearby boundaries in the inclination range that we could determine whether there are facets in the Wulff body at the (001) twist boundary inclinations and that these facets disappear on heating. We have not carried out such simulations.

The transitions we have seen at the $\Sigma 5$ and $\Sigma 29$ (001) twist boundaries bear some similarities to those discussed by Vitek *et al.*[12] They showed how sequences of different structural units at symmetric (210) and (310) tilt boundaries could be obtained by removing atoms, thus creating structures with periodicities larger than the primitive cell of the coincidence site lattice. In the limit these structures may become nonperiodic, but they still display short-range order because everywhere they are locally characterized by a small number of defined structural unit configurations. At absolute zero these boundary configurations may have very similar energies, giving rise to the concept of multiplicity of structures.[13] At low temperatures it was envisaged that ordered sequences of structural units would exist. As the temperature is raised the populations of structural units that may appear in a particular boundary was predicted[12] to change to minimize the boundary free energy. It was envisaged that in general these changes would be effected by variations in the vacancy content of the boundary. Although we have found that removal of atoms from twist boundaries is crucial for obtaining ground-state structures of these boundaries, our simulations of heating these boundaries to T_M are carried out at constant number of atoms in the boundary. In principle atoms could be exchanged between the boundaries and the free surfaces in our simulations, but in practice the free surfaces are too far from the boundaries for this to occur over the duration of our molecular dynamics simulations. In reality boundaries usually do have the freedom to exchange matter with the adjoining crystals, as envisaged in Ref. 12. A simulation that allowed this more realistic exchange of matter during annealing would require a grand canonical Monte Carlo approach, as in Ref. 14.

V. CONCLUSIONS

(001) twist boundaries in silicon display elements of structural order at all temperatures up to the bulk melting point. There is no premelting and no transition to an amorphous state on heating.

For two large angle twist boundaries continuous disordering transitions are seen, resulting in complete disorder only at the bulk melting point. These transitions are effected through local fluctuations between ordered and disordered states of the boundary, the frequency of which increases with temperature. However, even at temperatures just below the bulk melting point well defined structural units have a transitory existence for some 10 ps. These boundaries retain a memory of their low temperature states even at temperatures just below T_M. Greater structural order is retained at all temperatures in the small angle twist boundary, although there is evidence of a continuous structural transition below T_M, which nevertheless results in a finite boundary width at all temperatures up to T_M.

ACKNOWLEDGMENTS

S.v.A. and K.K. acknowledge the support of the Academy of Finland under the Finnish Centre of Excellence Programme 2006-2011 (Project No. 123470, Computational Complex Systems Research). A.P.S. acknowledges the support of the European Commission under Contract No. NMP3-CT-2005-013862 (INCEMS), and the support of a Royal Society Wolfson Merit Award.

[1] A. P. Sutton and R. W. Balluffi, *Interfaces in Crystalline Materials* (Oxford University Press, New York, 1995).
[2] M. Tang, W. C. Carter, and R. M. Cannon, Phys. Rev. B **73**, 024102 (2006).
[3] S. von Alfthan, P. D. Haynes, K. Kaski, and A. P. Sutton, Phys. Rev. Lett. **96**, 055505 (2006).
[4] S. von Alfthan, K. Kaski, and A. P. Sutton, Phys. Rev. B **74**, 134101 (2006).
[5] J. Tersoff, Phys. Rev. B **38**, 9902 (1988).
[6] P. Keblinski, D. Wolf, S. R. Phillpot, and H. Gleiter, Philos. Mag. Lett. **76**, 143 (1997).
[7] S. Nosé, J. Chem. Phys. **81**, 511 (1984).
[8] P. R. ten Wolde, M. J. Ruiz-Montero, and D. Frenkel, Phys. Rev. Lett. **75**, 2714 (1995).
[9] A. P. Sutton and V. Vitek, Philos. Trans. R. Soc. London, Ser. A **309**, 1 (1983).
[10] P. Keblinski, S. R. Phillpot, and D. Wolf, J. Am. Ceram. Soc. **80**, 177 (1997).
[11] A. Hedler, S. L. Klaumünzer, and W. Wesch, Nat. Mater. **3**, 804 (2004).
[12] V. Vitek, Y. Minonishi, and G.-J. Wang, J. Phys. Colloq. **46**, C4 (1985).
[13] G.-J. Wang, A. P. Sutton, and V. Vitek, Acta Metall. **32**, 1093 (1984).
[14] T. S. Hudson, D. Nguyen-Manh, A. C. T. van Duin, and A. P. Sutton, Mater. Sci. Eng., A **422**, 123 (2006).